Available online at www.sciencedirect.com
ScienceDirect
Bioelectrochemistry 69 (2006) 172 – 179
Bioelectrochemistry
www.elsevier.com/locate/bioelechem

Selectivity and sensitivity of a reagentless electrochemical DNA sensor studied by square wave voltammetry and fluorescence

Steeve Reisberg, Benoît Piro, Vincent Noel, Minh Chau Pham *

Laboratoire Interfaces–Traitements–Organisation et Dynamique des Systèmes (ITODYS). Université Paris 7–Denis Diderot, associé au CNRS, UMR 7086, 1, rue Guy de la Brosse, 75005 Paris, France

Received 21 September 2005; received in revised form 19 December 2005; accepted 30 December 2005
Available online 6 March 2006

Abstract

Poly(5-hydroxy-1,4-naphthoquinone-co-5-hydroxy-3-thioacetic acid-1,4-naphthoquinone)-modified electrode is used for the direct electrochemical detection of oligonucleotide hybridization. The polymer film presents well-defined electroactivity in the cathodic potential domain (between 0 and −0.8 V/SCE), due to the quinone group embedded into the polymer structure. The detection can be performed simply by square wave voltammetry. This sensor is a "signal-on" device and works with different oligonucleotide lengths, from 10 to 30 bases. Quantitative results from fluorescence are consistent with electrochemical data. It is confirmed that the signal increase in square wave voltammetry is unambiguously due to hybridization. The biosensor presents a detection limit of target of ca. 25 nM and is highly selective as it can discriminate single mismatch base.

Keywords: Oligonucleotide; Conducting polymer; Electrochemical hybridization sensor; Reagentless detection

1. Introduction

Numerous DNA sensors have been reported in the literature in the recent years. These systems can be classified into three generations of sensors, from the most complicated to the simplest one.

The "first generation" of DNA sensors need a chemical labeling of the target DNA. Labels are fluorescent [1–3], radioactive [4,5], electroactive molecules [6–8], enzymes [9–11], or electroactive molecules together with enzyme [12]. Radioactive and fluorescent labeling are reliable and very sensitive, but imply heavy instrumentation. Electroactive labeling is interesting as low equipment is needed, however sensitivity is lower.

The "second generation" of DNA sensors do not require chemical modification of the target strand, but need a reagent to be added in solution. Again, fluorescent molecules can be interesting, while recognizing selectively double-stranded ODN (dsODN) [13]. Colorimetric methods based on nanoparticles are also of great interest, and ultra-sensitive [14,15]. In the field of electrochemistry, one can find the use of mediators for the electrochemical oxidation of nucleobases [16–18], small redox indicators presenting a specific affinity with single or double strands [18–22] or redox polymers added in solution [23]. Adsorptive stripping voltammetry (ASV), combined with redox indicators, allow to enhance sensitivity [24,25]. 'Sandwich' structures [26,27] constitute also an interesting method but one of the most innovative techniques relates the use of metal or semiconductor nanoparticles [25,28,29].

The "third generation" concerns reagentless DNA sensors. They do not need modification of the target, neither addition of a reagent to detect hybridization. Among them, one finds of course surface plasmon resonance (SPR) [30,31], piezoelectric systems [32], but also, again, electrochemical techniques as adsorptive stripping voltammetry [33–35], impedance spectroscopy [36] or methods based on "smart" electrodes, as conducting polymer-modified electrodes [37–43].

In the literature, all the works dealing with electrically conducting polymers (ECPs) report a signal decrease following hybridization, i.e. a "signal-off" detection. Conversely, our electrochemical sensor presents a "signal-on" detection.

* Corresponding author. Tel.: +33 1 44276961; fax: +33 1 44276814.
E-mail address: mcpham@paris7.jussieu.fr (M.C. Pham).

1567-5394/$ - see front matter © 2006 Elsevier B.V. All rights reserved.
doi:10.1016/j.bioelechem.2005.12.007

Previous results were published, to describe the sensor [44], followed by an original work showing that the signal depends on the probe sequence localization [45]. It was assumed that the "signal-on" behavior was due to the cation-exchange process of the transducer which is the quinone group embedded in poly(5-hydroxy-1,4-naphthoquinone-co-5-hydroxy-3-thioacetic acid-1,4-naphthoquinone) film (called poly(JUG-co-JUGA) in the following). This is opposite to the case of classical conducting polymers (polyaniline, polypyrrole, and polythiophene) where the transduction was performed by the redox process of the polymer exchanging anions.

In this paper, the purpose is first to demonstrate clearly and unambiguously that the signal increase is due to the hybridization event. For that, each electrochemical experiment is supported by a fluorescence analysis, performed under the same experimental conditions. This allows to detect hybridization both qualitatively and quantitatively.

Secondly, hybridization results are discussed as a function of the probe and target length. It is shown that hybridization with 10-, 20- and 30-base target sequences respectively onto 17-, 27- and 37-base probe strands is very selective in all cases. The biosensor can discriminate not only a random sequence, but also a double mismatch and a single mismatch. Our system allows then to evidence punctual mutations. In particular, substitution of a puric base by a pyrimidic base (case of the mismatch in the MCHIV strand), called a *transversion* and known to be difficult to detect [46,47], is clearly discriminated herein.

Thirdly, in the case of hybridization of the 20-base target onto the 27-base probe, the current variation is discussed as a function of the target concentration. This allows to determine the detection limit of our sensor.

2. Experimental section

2.1. Chemicals

N′-(3-dimethylaminopropyl)-*N*-ethylcarbodiimide hydrochloride (EDC) and *N*-hydroxysuccinimide (NHS) were provided by Sigma. Phosphate-buffered saline (PBS; 0.137 M NaCl, 0.0027 M KCl, 0.0081 M Na_2HPO_4, 0.00147 M KH_2PO_4, pH 7.4) was from Sigma. Aqueous solutions were made with bi-distilled or ultrapure (Millipore) water. Juglone (JUG) and 1-naphthol (1-NAP) were purchased from Fluka. 5-hydroxy-3-thioacetic acid-1,4-naphthoquinone (JUGA) was synthesized in the lab [44]. Acetonitrile (ACN) was supplied by Aldrich (HPLC grade). All other reagents used were of analytical grade. Oligonucleotides were synthesized by MWG Biotech (Germany) and are detailed herein (bases really used in bold, mismatches underlined). Probe sequences are: SHORT (17-mer, 5′-TC-**CTC TCC TTC T**-AGCCT-3′C_7NH_2), GEM (27-mer, 5′-TC-**GCA CCC ATC TCT CTC CTT CT**-AGCCT-3′C_7NH_2) and GEMC (37-mer, 5′-TC-**CCT CAT AGT CGC ACC CAT CTC TCT CCT TCT**-AGCCT-3′C_7NH_2). Complementary targets are respectively A (10-mer, 3′-GAG AGG AAG A-5′), HIV (20-mer, 3′-CGT GGG TAG AGA GAG GAA GA-5′) and CHIV (30-mer, 3′-GGA GTA TCA GCG TGG GTA GAG AGA GGA AGA-5′). Mismatching sequences are respectively MHIV (20-mer, one mismatch, 3′-CGT GGG TAA AGA GAG GAA GA-5′), M′HIV (20-mer, one mismatch, 3′-CGT GGG TAG AGA GAT GAA GA-5′), 2MHIV (20-mer, two mismatches, 3′-CGT GGG TAA AGA GAT GAA GA-5′), MCHIV (30-mer, one mismatch, 3′GGA GTA TCA GCG TGG GTA GAG AGA TGA AGA 5′), M′CHIV (30-mer, one mismatch, 3′ GGA GTA TCA GCG TGG GTA AAG AGA GGA AGA 3′) and 2CHIV (30-mer, two mismatches, 3′ GGA GTA TCA GCG TGG GTA AAG AGA TGA AGA 5′). Random sequences are RANDA (10-mer, 3′-TCC GCC TAA G-5′), RAND (20-mer, 3′-ATC CAT GCA TTC CGC CTA AG-5′) and RANDC (30-mer, 3′ TTG AAC CAG TAT CCA TGC ATT CCG CCT AAG 5′).

Probe grafting was performed as follows. Poly(JUG-co-JUGA)-coated glassy carbon (GC) electrodes were dipped into a solution containing 0.1 μM of probe (SHORT, GEM or GEMC), 1.5×10^{-2} M EDC (3×10^{-5} mol, 1 Eq) and 3×10^{-2} M NHS (6×10^{-5} mol, 2 Eq) in distilled water at 37 °C. After 20 h, the ODN immobilization reaction was stopped: the electrode was washed with distilled water (5 min) in order to remove non-covalently bound ODN, then with PBS (2 h at 37 °C). Phosphates in PBS are able to react with NHS-activated ester. As a consequence, unreacted ester groups are removed.

2.2. Electrochemical methods

For electrochemical experiments, a conventional one-compartment, three-electrode cell was employed. An EG&G 263A potentiostat was used with the Echem software (Ecochemie). The working electrodes were glassy carbon disks (Tokaï) of 0.07 cm^2 area or GC plates of 2 cm^2 (for fluorescence experiments). The auxiliary electrode was a platinum grid and the reference electrode a commercial Saturated Calomel Electrode (SCE).

The electrochemical synthesis of poly(JUG-co-JUGA) films was carried out by electrooxidation of a mixture of 5×10^{-2} M JUG + 5×10^{-3} M JUGA + 2×10^{-3} M 1-naphthol + 0.1 M $LiClO_4$ in acetonitrile, on GC electrodes, under dried argon atmosphere, by potential scans from 0.4 to 1 V vs. SCE during 50 cycles at 50 mV s^{-1}. Electrochemical synthesis and film characterizations were described elsewhere [48].

Hybridization was detected by recording the modification of the redox process of the quinone group, using square wave voltammetry (SWV). The following parameters were used: pulse height 50 mV, pulse width 50 ms, scan increment 2 mV, frequency 12.5 Hz, potential domain (−0.8; 0 V vs. SCE). The medium was PBS, bubbled with argon for 40 min before and during SWV measurements. The SWV scans were repeated until complete stabilization of the signal (i.e., no difference observed between two successive responses). All electrochemical experiments were conducted at 25 °C.

2.3. Hybridization

For hybridization experiments, solutions containing 0.1 μM target (A, RANDA, HIV, MHIV, M′HIV, 2MHIV, RAND,

CHIV, MCHIV, M′CHIV, 2MCHIV or RANDC) in PBS (pH=7.4) were used. The electrode bearing the probe strand was dipped in the target solution then heated at a temperature above the melting temperature of the duplex during 2 h, and slowly cooled down to room temperature (at a rate of 0.5 °C/min down to 25 °C). After that, the electrode was washed in PBS for 1 h at 25 °C in order to remove the non-hybridized strands.

2.4. Fluorescence experiments

The apparatus used is an Aminco-Bowman Series 2 spectrophotofluorometer. Fluorescent targets are modified with a BODIPY® 650/675 molecule (from Molecular Probes, provided by MWG Biotech) on their 5′-end. The excitation wavelength is 650 nm, and the emission wavelength 675 nm. Marked ODN are noted in the following with an asterisk (*). We used A*, RANDA*, HIV*, RAND*, CHIV*, MHIV*, M′HIV* or RANDC*, following strictly the same hybridization protocol than for the unlabelled targets, using 2 cm^2 GC plates instead of 0.07 cm^2 GC disks. To quantify hybridization of these target strands onto the immobilized probe strands, a washing sequence was systematically followed, in four steps. The three first steps consist in soaking the film in a volume of 2 mL (V) of PBS, at 25 °C, under magnetic stirring, during 5 min (step 1), 10 more min (step 2), and 30 more min (step 3). After each step, the 2 mL solution is taken, stored for subsequent fluorescence experiments, and replaced by a fresh one. After these extensive washing steps, the fourth treatment consists in soaking the film in 2 mL of pure water at 80 °C during 10 min. Under these stringent conditions, it can be assumed that all hybrids present on the film are denatured, and the target strand withdrawn. The target strands are therefore released in solution, which is removed and stored for subsequent fluorescence experiments. To determine the ODN concentration in these samples, calibration curves were first obtained, for each fluorescent strand (in the range 0.25–10 nM). ODN concentrations (C, mol L^{-1}) were then converted into ODN surface concentrations (Γ, mol cm^{-2}) following the simple formula: $\Gamma = C \times V \times S^{-1}$. Surface concentrations are found in the 0–15 pmol cm^{-2} range.

2.5. XPS analysis

X-ray photoelectron spectroscopy (XPS) data were recorded on a Thermo VG Escalab 250 (Al anode). XPS signals were fitted with a sum of Gaussian (70%)/Lorenzian (30%) functions, and calibrated by assuming a 285 eV binding energy for aromatic and aliphatic carbons.

3. Results and discussion

3.1. SWV of poly(JUG-co-JUGA) film

Square wave voltammetry (SWV) was performed on a poly (JUG-co-JUGA)-modified electrode before treatment with the ODN probe (Fig. 1). The main SWV response (plain squares)

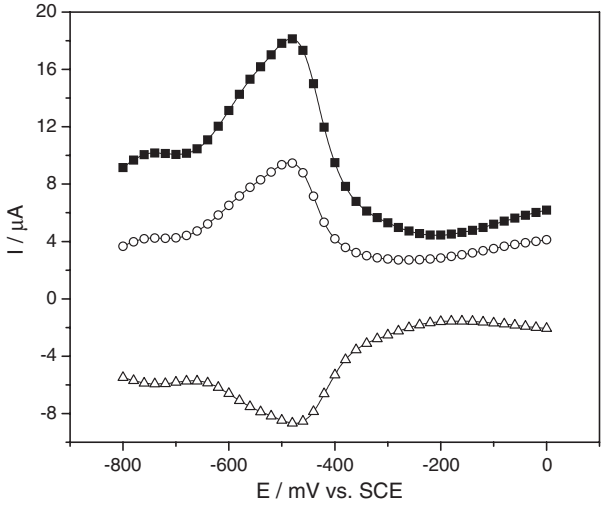

Fig. 1. SWV response (I_d) of a poly(JUG-co-JUGA)-modified GC electrode (plain squares), from −800 mV vs. SCE to 0 V vs. SCE (oxidation scan). Parameters: pulse height 50 mV, scan increment 2 mV, frequency 12.5 Hz. Medium: PBS. Electrode surface, S=0.07 cm^2. Open circles and open up-triangles correspond to the forward current (I_f) and the reverse current (I_r), respectively. $I_d = I_f - I_r$.

corresponds to a differential current I_d, that is the difference between a forward current (I_f, open circles) and a reverse current (I_r, open up-triangles). $I_d = I_f - I_r$. The potential was swept from −800 mV vs. SCE to 0 V vs. SCE (oxidation scan). Parameters: pulse height 50 mV, scan increment 2 mV, frequency 12.5 Hz. Medium: PBS. Electrode surface S=0.07 cm^2.

Two oxidation peaks appear in a range from −800 mV up to 0 V vs. SCE. The main peak presents a maximum at around −475 mV/SCE, and the second one appears as a shoulder at around −750 mV/SCE. These peaks correspond to the redox process of the quinone group [48]. In the following, it is the change in intensity of the most intense peak (centered at ca. −475 mV) that will be considered as significant for grafting and hybridization experiments.

3.2. Probe grafting

ODN probe strands were grafted onto poly(JUG-co-JUGA)-coated GC electrodes as described in the experimental section. The resulting films were analyzed by X-ray photoelectron spectroscopy (XPS) after ODN grafting. Typical elements that can be considered are C, N, S and P. Carbon is found in the nucleobases structure and in the background polymer layer, sulfur is found in the modified monomer JUGA, whereas nitrogen and phosphorus belong only to nucleobases and ODN backbone, respectively.

The C_{1s} spectrum (Fig. 2a) displays four peaks, at 285 eV, 286.4 eV, 287.9 eV and 289.3 eV. They can be respectively attributed to C–C and C=C (present in the polymer backbone and the nucleobases) (first peak), C–O, C–S and C–N (polymer backbone and ODN bases) (second peak), C=O (of the quinone group and in the bases) and C=N (of the bases) (third peak), and O–C=O, O–C=N or O=C–N (of the reacted and unreacted carboxylic group) (fourth peak).

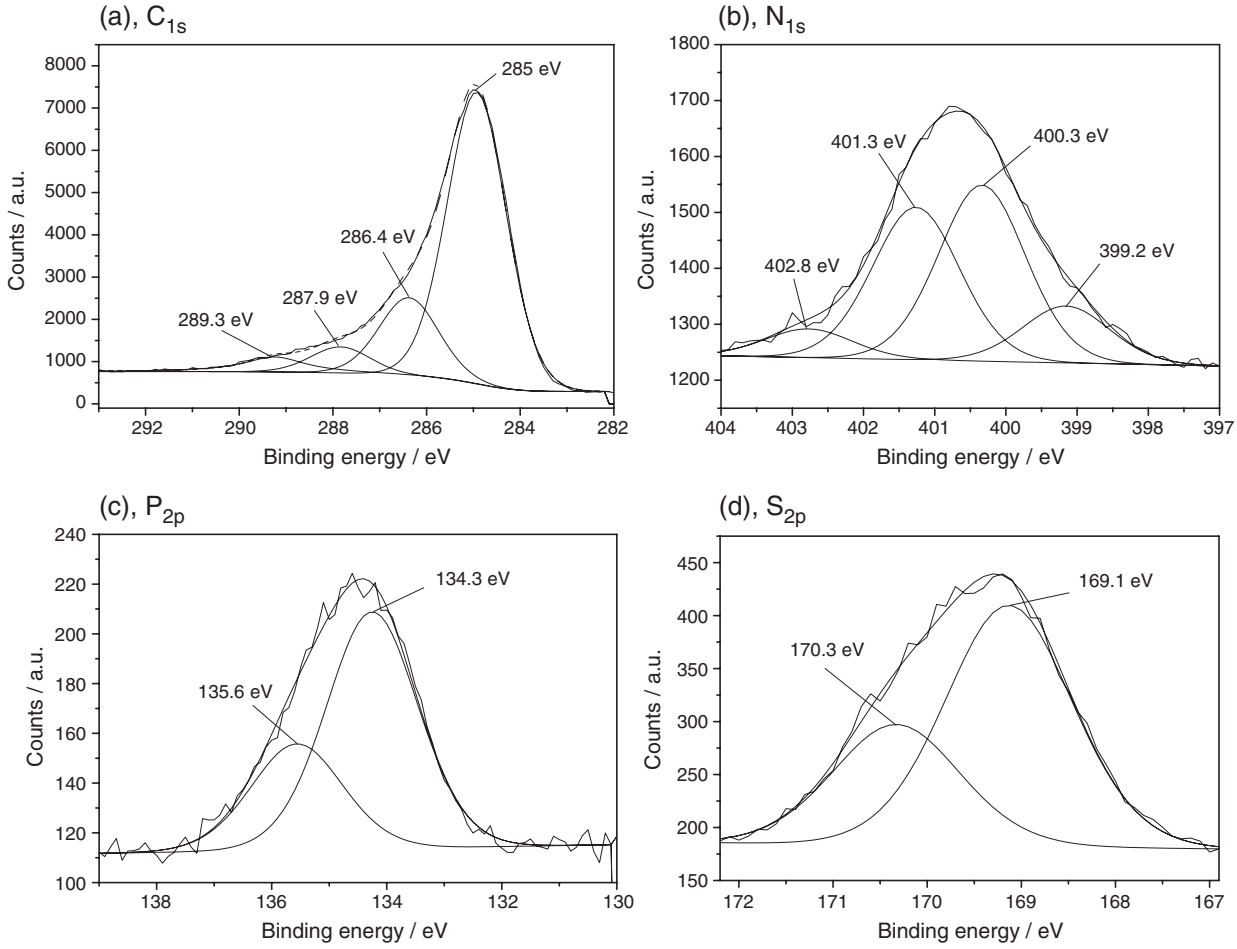

Fig. 2. XPS spectra of a poly(JUG-co-JUGA)/GC-modified electrode, onto which the a-GEM ODN probe is grafted. Spectra of: (a) C_{1s}; (b) N_{1s}; (c) P_{2p}; (d) S_{2p}.

The N_{1s} spectrum (Fig. 2b) displays also four peaks, at 399.2 eV, 400.3 eV, 401.3 eV and 402.8 eV. Nitrogen comes mainly from the nucleobases and from the peptide bond. Peaks at 399.2 eV and 400.3 eV can be attributed to the –N= in the heterocyclic bases whereas peaks at 401.3 eV and 402.8 eV can be attributed to the exocyclic amine group $–NH_2$ of the A, G and C nucleobases [49,50].

The P_{2p} spectrum (Fig. 2c) displays two peaks at 134.3 eV and 135.6 eV attributed to P $2p_{3/2}$ and P $2p_{1/2}$, respectively, corresponding to the phosphate groups of the ODN backbone [49].

The total peak surfaces for nitrogen and phosphorus are 1157 eV and 280 eV, using respectively, sensitivities of 1.8 and 1.2 for N and P. This gives a molar ratio P/N of 0.36, very close to the theoretical ratio (0.34) which can be calculated from the atomic composition of the a-GEM probe strand, i.e. 80 nitrogen and 27 phosphorus atoms. Phosphates in the PBS buffer are able to react with the remaining NHS-activated esters which were not transformed in peptide bond by ODN probes.

Fig. 2d shows the S_{2p} spectrum, which displays two peaks at 169.1 eV and 170.3 eV. This sulfur comes from the JUGA moieties in the polymer structure.

The experimental atomic ratios N/S and P/S are, respectively, equal to 1.4 and 0.5. If we make the hypothesis that each carboxylic function is involved in a peptide bond with an ODN, the theoretical ratios N/S and P/S are, respectively, 80 and 27. This probably indicates that the experimental proportion of

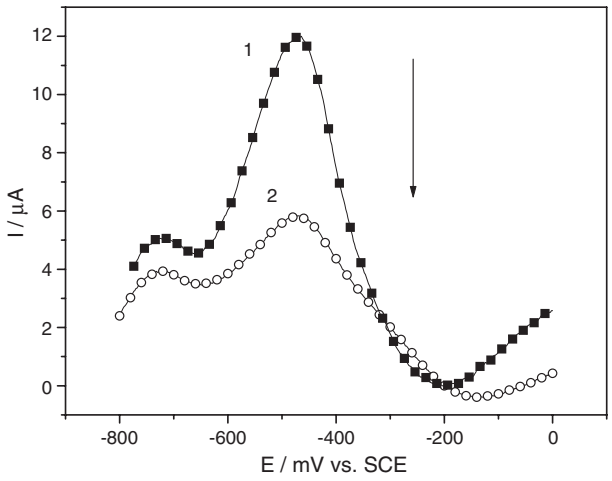

Fig. 3. SWV response of a naked poly(JUG-co-JUGA)-modified GC electrode (plain squares, curve 1), and of the same poly(JUG-co-JUGA)-modified GC electrode onto which the SHORT probe sequence is grafted (open circles, curve 2). SWV and grafting conditions described in the experimental section. S=0.07 cm^2. Medium: PBS. The background current at −0.2 V is subtracted.

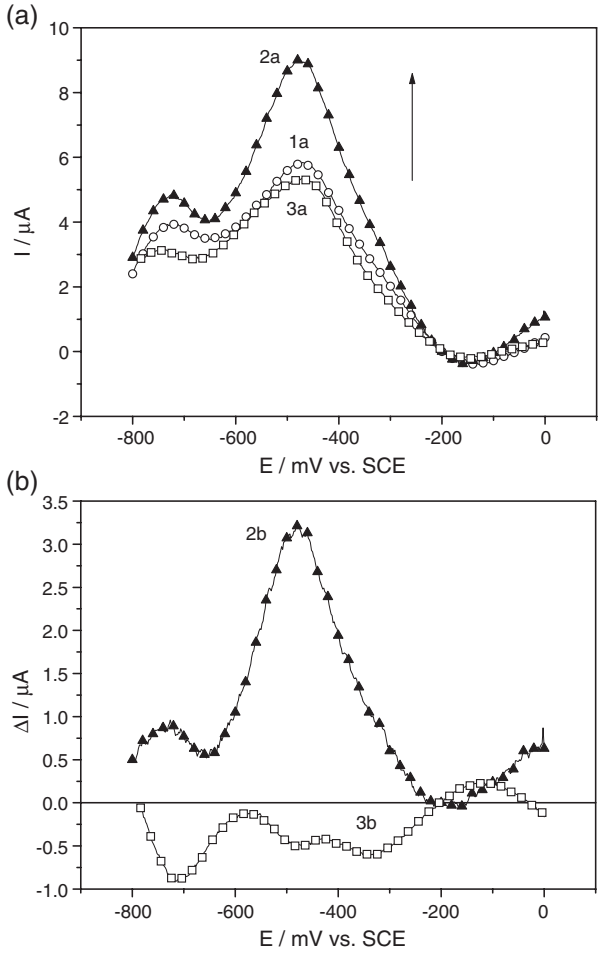

Fig. 4. (a) SWV response of a poly(JUG-co-JUGA)-modified GC electrode onto which the SHORT probe sequence is grafted (plain squares, curve 1a), after addition of A (plain down-triangles, curve 2a) or RANDA (open circles, curve 3a) targets. The background current at −0.2 V is subtracted. (b) Differential currents obtained by subtraction: curve (2b) corresponds to the current difference between curves (2a) and (1a), whereas curve (3b) corresponds to (3a)−(1a). [target]=100 nM. SWV conditions described in the experimental section. S=0.07 cm^2. Medium: PBS.

reacted carboxylic groups is 1.4/80, or 0.5/27, i.e. around 2%. This value is coherent with the probe density determined previously by radioactive labeling [44].

SWV was used to characterize the grafted film. The probe ODN a-GEM was grafted as described above. The current intensity is high for the unmodified film (before grafting), and diminishes after ODN probe grafting. This behavior is well illustrated on Fig. 3, with the SHORT probe (10+7 bases), before grafting (curve 1, plain squares) and after grafting (curve 2, open circles). Similar behavior is observed with GEM (20+7 bases) and GEMC (30+7 bases) probes (not shown).

3.3. Hybridization with 10-base probe and target

SWV was performed on a poly(JUG-co-JUGA)-modified electrode onto which the SHORT probe (10 used bases, 5 unused bases as spacer after the 3′-amino-C7 modifier, and 2 unused bases on the 5′-end to avoid edge effect) is grafted (sequences detailed in the experimental section). Target A (full complementary) or RANDA (random) is then added (Fig. 4a). Curve (1a) corresponds to the SWV response of the electrode onto which the SHORT probe is grafted, curve (2a) after addition of the complementary sequence A, and curve (3a) after addition of the RANDA sequence. These results are presented differently on Fig. 4b, as current differences. Curve (2b) corresponds to the current difference between curves (2a) and (1a), whereas curve (3b) corresponds to (3a)−(1a). SWV experiments conducted in the following will be presented under this format (differential curves). As shown, the RANDA target sequence does not lead to a significant current change, whereas A leads to a strong increase in signal.

These results were supported by quantitative measurements, performed by fluorescence spectroscopy, as detailed in the experimental section. The results are reported in Fig. 5.

As shown, the A* strand is weakly adsorbed on the film surface, but it can be washed off by a simple soaking of the film in PBS, at 25 °C, during ~15 min (first and second washing steps). The total amount of adsorbed A* is 1.9±0.4 pmol cm^{-2}, whereas that of RANDA* is 0.7±0.4 pmol cm^{-2}. The higher quantity concerning A* is probably due to the fact that some A* strands dehybridize during these washing steps. At the third washing step, negligible quantities are desorbed. The fourth washing step is much more severe. The film is soaked during 10 min in pure hot water (80 °C, far above the melting temperature of the double strand) in order to denature all hybrids. This leads to dehybridization of a quantity of ODN* that is equivalent to 2.6±0.5 pmol cm^{-2} for the complementary strand A*, and to a negligible amount for the random sequence RANDA*. This shows a very good selectivity of the 17-base probe strand (SHORT) towards the 10-base targets.

These results demonstrate that the hybridization is truly responsible for the current increase, whereas the addition of the RANDA* strand, which does not hybridize, leads to a negligible current change.

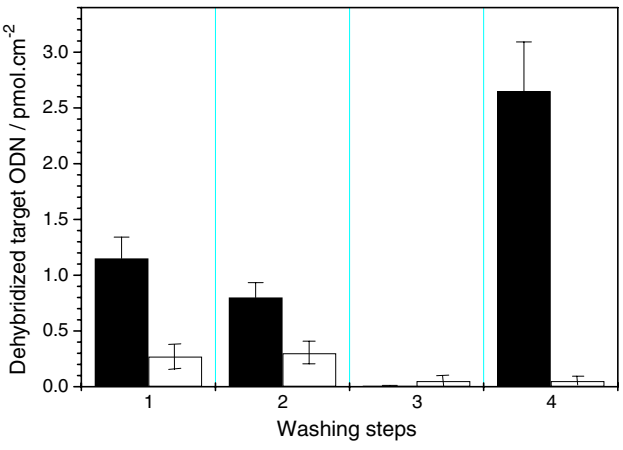

Fig. 5. Target ODN surface concentration measured after: 1) washing in PBS at 25 °C during 5 min; 2) washing in PBS at 25 °C during 10 more min; 3) washing in PBS at 25 °C during 30 more min; 4) washing in pure water at 80 °C during 15 min. Left (black): full complementary A*; Right (white): random sequence RANDA*.

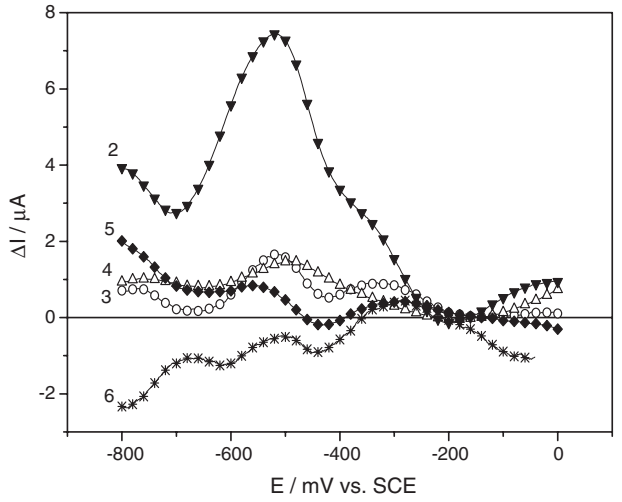

Fig. 6. Differential currents obtained by subtraction of the SWV responses of the electrode onto which the GEM probe is grafted (zero reference), after addition of HIV (curve 2, plain down-triangles), MHIV (curve 3, open circles), RAND (curve 4, open up-triangles), M′HIV (curve 5, plain diamond) and 2MHIV (curve 6, stars) targets. Same conditions as Fig. 4.

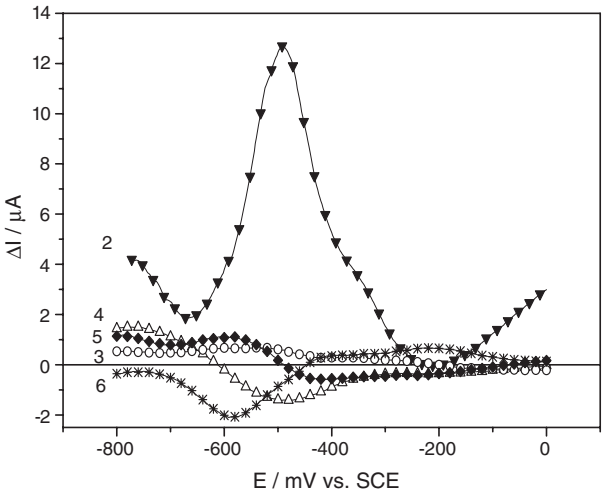

Fig. 8. Differential currents obtained by subtraction of the SWV responses of the electrode onto which the GEM probe is grafted (zero reference), after addition of CHIV (curve 2, plain down-triangles), MCHIV (curve 3, open circles), RANDC (curve 4, open up-triangles), M′CHIV (curve 5, plain diamond) and 2MCHIV (curve 6, stars) targets. Same conditions as Fig. 4.

3.4. Hybridization with 20-base probe and target

It is shown above that hybridization of the 10-base target is selective, and leads to a measurable current change.

SWV experiments were extended to the 27-base probe GEM and different 20-base targets (Fig. 6): HIV (full complementary), MHIV and M′HIV (single mismatch sequences), 2MHIV (double mismatches sequence) or RAND (random). Curve 2 corresponds to the SWV response of the electrode onto which the GEM probe is grafted. Addition of the M′HIV sequence (mismatch positioned near the 3′-end of the probe, curve 5) does not lead to any significant signal change. For MHIV (mismatch positioned near the 5′-end of the probe, curve 3), as for the random sequence RAND (curve 4), the current increases slightly (1.5 μA at −500 mV), but corresponds to only 20% of the current recorded for the full-complementary HIV. The double-mismatch sequence 2MHIV leads to a slight current decrease (curve 6, 0.5 μA at −500 mV).

As done for the 10-base SHORT probe, hybridization was quantified with fluorescent targets HIV*, MHIV*, M′HIV*, 2MHIV* and RAND*. The results are reported in Fig. 7. The approach is the same than the one followed for the SHORT/A hybrid. The experimental protocol consists in 3 washing steps (1 → 3), followed by a dehybridization step (4). As for the 10-base target, adsorption is very low (no more than a total of 4 ± 0.4 pmol cm^{-2} for the complementary strand). It is also obvious that hybridization is very selective in these conditions, with this 20-base target sequence. Ca. 13 ± 1 pmol cm^{-2} of HIV* hybridizes, while none of the non-complementary strands

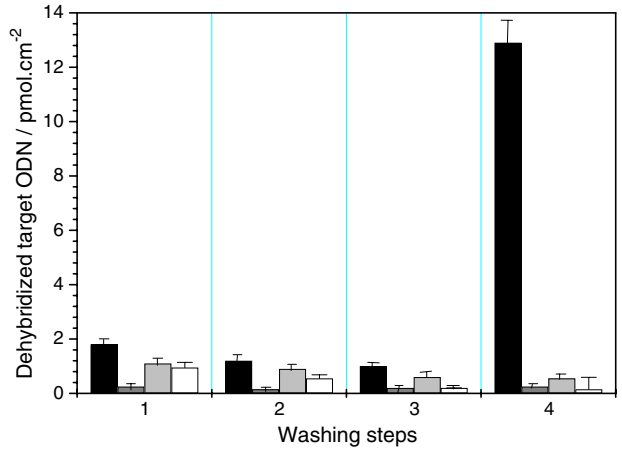

Fig. 7. Target ODN surface concentration measured after: 1) washing in PBS at 25 °C during 5 min; 2) washing in PBS at 25 °C during 10 more min; 3) washing in PBS at 25 °C during 30 more min; 4) washing in pure water at 80 °C during 15 min. From left to right: full complementary HIV*, MHIV*, M′HIV* and RAND*.

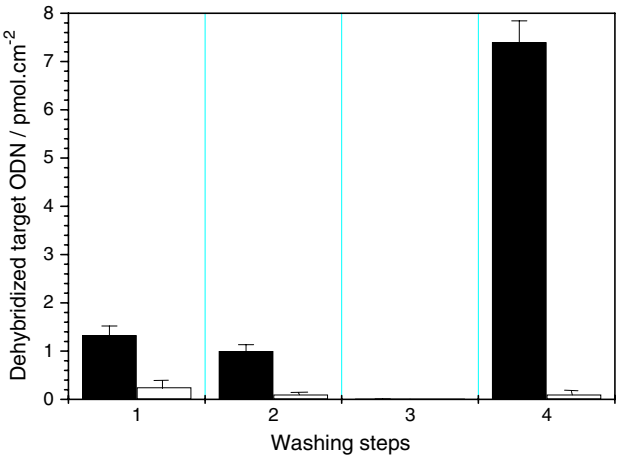

Fig. 9. Target ODN surface concentration measured after: 1) washing in PBS at 25 °C during 5 min; 2) washing in PBS at 25 °C during 10 more min; 3) washing in PBS at 25 °C during 30 more min; 4) washing in pure water at 80 °C during 15 min. Left: full complementary CHIV*; Right: random sequence RANDC*.

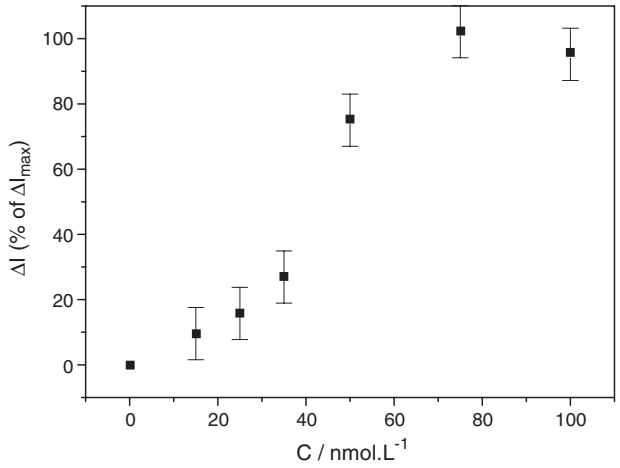

Fig. 10. Differential currents (percentage of the maximum at 75 nM), measured at −500 mV/SCE, after addition of HIV (20-mer complementary target), for increasing concentrations from 15 nM up to 100 nM. Same conditions as Fig. 4.

hybridizes (Fig. 7). It must also be stressed that the adsorption level remains exceptionally low. This is a very positive point, because no "artificial" anti-adsorption agent (bovine serum albumin, non-specific DNA, etc.) has to be used. In addition, transition or transversion (substitution of puric and pyrimidic bases), known to be difficult to detect, are clearly discriminated herein.

3.5. Hybridization with 30-base probe and target

Experiments were extended to a 30-base probe (GEMC) and various 30-base targets (the complementary one, CHIV; a random sequence, RANDC; two single mismatches, MCHIV and M′HIV; and 2MCHIV containing two mismatches). As shown (Fig. 8), the SWV peak current increases selectively only after addition of the complementary strand (~+13 μA). For the other strands, the current variations are negligible.

As for the other strands lengths, we determined by fluorescence the quantity of ODN adsorbed or hybridized. For costs reason, only CHIV* and RANDC* were used. As shown on Fig. 9, non-specific adsorption is low (2.4±0.4 pmol cm^{-2} maximum) for CHIV*, and near zero for RANDC*. As for the 10- and 20-base sequences, this is probably due to dehybridization of some CHIV* sequences during the washing steps. On the contrary, CHIV* hybridizes with a surface concentration of ca. 7.4±0.4 pmol cm^{-2}. Again, from these results, the current increase on Fig. 8 can be unambiguously attributed to hybridization of CHIV on the immobilised probe strand.

3.6. Effect of target concentration

The SWV current response was measured as a function of the concentration of target strand. This experiment was made with the 27-base GEM probe sequence and the 20-base target strand HIV. The results are shown on Fig. 10, for concentrations between 15 nM and 100 nM. It appears that the current response remains low (compared to the experimental error) for target concentrations below 25 nM, then follows a sharp increase until a maximum reached above 60 nM. This detection limit of 25 nM can be advantageously compared to most of the results published in the literature on DNA sensor using conducting polymer as the transduction element [37–43].

It must be kept in mind that our electrode bears around 10 pmol cm^{-2} of ODN probe, for a surface of 0.07 cm^2. Therefore, the lowest "theoretical" target strand amount we can detect here is probably around 700 fmol (one target for one probe). This limit can be even lower if the electrode area is decreased. This is theoretically possible as the sensor delivers relatively high current densities.

4. Conclusion

We have shown in this work that hybridization of ODN can be directly detected by a "signal-on" detection in square wave voltammetry curves on a poly(JUG-co-JUGA)-modified electrode. This reagentless sensor can be used for different ODN lengths, from 10 bases up to 30 bases. Each time, hybridization leads to a current increase when the full-complementary strand is added, whereas negligible changes occur with non-complementary or mismatching sequences (transitions, transversions). This demonstrates the high selectivity of this bioelectrode. For each system, hybridization is quantitatively controlled by fluorescence experiments. The target concentration is also varied to evaluate the electrode sensitivity.

Acknowledgment

S.R. thanks the French Ministry of Research for a Ph.D. grant.

References

[1] S. Fodor, J.L. Read, M.C. Pirrung, L. Stryer, A. Tsai Lu, D. Solas, Light-directed, spatially addressable parallel chemical synthesis, Science 251 (1991) 767–773.
[2] J.R. Epstein, I. Biran, D.R. Walt, Fluorescence-based nucleic acid detection and microarrays, Anal. Chim. Acta 469 (2002) 3–36.
[3] T. Livache, A. Roget, E. Dejean, C. Barthet, G. Bidan, R. Teoule, Preparation of a DNA matrix via an electrochemically directed copolymerization of pyrrole and oligonucleotides bearing a pyrrole group, Nucleic Acids Res. 22 (1994) 2915–2921.
[4] Y. Okahata, Y. Matsunobu, K. Ijiro, M. Mukae, A. Murkami, K. Makino, Hybridization of nucleic acids immobilized on a quartz crystal microbalance, J. Am. Chem. Soc. 114 (1992) 8299–8300.
[5] J. Wang, X. Cai, G. Rivas, H. Shiraishi, P.A.M. Farias, N. Dontha, DNA electrochemical biosensor for the detection of short DNA sequences related to the human immunodeficiency virus, Anal. Chem. 68 (1996) 2634–2969.
[6] E. Palecek, M. Fojta, F. Jelen, New approaches in the development of DNA sensors: hybridization and electrochemical detection of DNA and RNA at two different surfaces, Bioelectrochemistry 56 (2002) 85–90.
[7] M. Fojta, L. Havran, S. Billova, P. Kostecka, M. Masarik, R. Kizek, Two-surface strategy in electrochemical DNA hybridization assays: detection of osmium-labeled target DNA at carbon electrodes, Electroanalysis 15 (2003) 431–440.
[8] A. Anne, A. Bouchardon, J. Moiroux, 3′-Ferrocene-labeled oligonucleotide chains end-tethered to gold electrode surfaces: novel model systems for exploring flexibility of short DNA using cyclic voltammetry, J. Am. Chem. Soc. 125 (2003) 1112–1113.

[9] T. de Lumley-Woodyear, C.N. Campbell, A. Heller, Direct enzyme-amplified electrical recognition of a 30-base model oligonucleotide, J. Am. Chem. Soc. 118 (1996) 5504–5505.
[10] F. Azec, C. Grossiord, M. Joannes, B. limoges, P. Brossier, Hybridization assay at a disposable electrochemical biosensor for the attomole detection of amplified human cytomegalovirus DNA, Anal. Biochem. 284 (2000) 107–113.
[11] J. Wang, A.N. Kawde, M. Musameh, G. Rivas, Dual enzyme electrochemical coding for detecting DNA hybridization, Analyst 127 (2002) 1279–1282.
[12] F. Patolsky, Y. Weizmann, I. Willner, Redox-active nucleic-acid replica for the amplified bioelectrocatalytic detection of viral DNA, J. Am. Chem. Soc. 124 (2002) 770–772.
[13] F.F. Bier, F.W. Scheller, Label-free observation of DNA-hybridization and endonuclease activity on a wave guide surface using a grating coupler, Biosens. Bioelectron. 11 (1996) 669–674.
[14] J. Liu, Y. Lu, Colorimetric biosensors based on DNAzyme-assembled gold nanoparticles, J. Fluoresc. 14 (2004) 343–354.
[15] C.A. Mirkin, R.L. Letsinger, R.C. Mucic, J.J. Storhoff, A DNA-based method for rationally assembling nanoparticles into macroscopic materials, Nature 382 (1996) 607–609.
[16] I.V. Yang, H.H. Thorp, Modification of indium tin oxide electrodes with repeat polynucleotides: electrochemical detection of trinucleotide repeat expansion, Anal. Chem. 73 (2001) 5316–5322.
[17] P.M. Armistead, H.H. Thorp, Electrochemical detection of gene expression in tumor samples: overexpression of Rak nuclear tyrosine kinase, Bioconjug. Chem. 13 (2002) 172–176.
[18] B. Wang, L. Bouffier, M. Demeunynck, P. Mailley, A. Roget, T. Livache, P. Dumy, New acridone derivatives for the electrochemical DNA-hybridization labelling, Bioelectrochemistry 63 (2004) 233–237.
[19] K.M. Millan, S.R. Mikkelsen, Sequence-selective biosensor for DNA based on electroactive hybridization indicators, Anal. Chem. 65 (1993) 2317–2323.
[20] A.B. Steel, T.M. Herne, M.J. Tarlov, Electrochemical quantitation of DNA immobilized on gold, Anal. Chem. 70 (1998) 4670–4677.
[21] M.V. Del Pozo, C. Alonso, F. Pariente, E. Lorrenzo, Electrochemical DNA sensing using osmium complexes as hybridization indicators, Biosens. Bioelectron. 20 (2005) 1549–1558.
[22] A.M. Oliveira-Brett, M. Vivan, I.R. Fernandes, J.A.P. Piedade, Electrochemical detection of in situ adriamycin oxidative damage to DNA, Talanta 56 (2002).
[23] A. Liu, J.I. Anzai, Use of polymeric indicator for electrochemical DNA sensors: poly(4-vinylpyridine) derivative bearing [*Os*(5,6-dimethyl-1,10-phenanthroline)$_2$Cl]$^{2+}$, Anal. Chem. 76 (2004) 2975–2980.
[24] G. Marrazza, I. Chianella, M. Mascini, Disposable DNA electrochemical sensor for hybridization detection, Biosens. Bioelectron. 14 (1999) 43–51.
[25] J. Wang, D. Xu, A. Kawde, R. Polsky, Metal nanoparticle-based electrochemical stripping potentiometric detection of DNA hybridization, Anal. Chem. 73 (2001) 5576–5581.
[26] R.M. Umek, S.W. Lin, J. Vielmetter, R.H. Terbrueggen, B. Irvine, C.J. Yu, J.F. Kayyem, H. Yowanto, G.F. Blackburn, D.H. Farkas, Y.P. Chen, Electronic detection of nucleic acids: a versatile platform for molecular diagnostics, J. Mol. Diag. 3 (2001) 74–84.
[27] E. Dominguez, O. Rincon, A. Narvaez, Electrochemical DNA sensors based on enzyme dendritic architectures: an approach for enhanced sensitivity, Anal. Chem. 76 (2004) 3132–3138.
[28] E. Katz, I. Willner, J. Wang, Electroanalytical and bioelectroanalytical systems based on metal and semiconductor nanoparticles, Electroanalysis 16 (2004) 19–43.
[29] J. Wang, Nanomaterial-based electrochemical biosensors, The Analyst 130 (2005) 421–426.
[30] R.J. Heaton, A.W. Peterson, R.M. Georgiadis, Electrostatic surface plasmon resonance: direct electric field-induced hybridization and denaturation in monolayer nucleic acid films and label-free discrimination of base mismatches, Proc. Natl. Acad. Sci. 98 (2001) 3701–3704.
[31] T. Livache, P. Guedon, C. Brakha, A. Roget, Y. Levy, G. Bidan, Polypyrrole electrospotting for the construction of oligonucleotide arrays compatible with a surface plasmon resonance hybridization detection, Synth. Met. 121 (2001) 1443–1444.
[32] T. Tatsuma, Y. Watanabe, N. Oyama, K. Kitakizaki, M. Haba, Multichannel quartz crystal microbalance, Anal. Chem. 71 (1999) 3632–3636.
[33] E. Palecek, Adsorptive transfer stripping voltammetry: determination of nanogram quantities of DNA immobilized at the electrode surface, Anal. Biochem. 170 (1988) 421–431.
[34] E. Palecek, Preface, Talanta 56 (2002) 809–819.
[35] D. Ozkan, A. Erdem, P. Kara, K. Kerman, B. Meric, J. Hassmann, M. Ozsoz, Allele-specific genotype detection of factor V Leiden mutation from polymerase chain reaction amplicons based on label-free electrochemical genosensor, Anal. Chem. 74 (2002) 5931–5936.
[36] E. Souteyrand, J.P. Cloarec, J.R. Martin, C. Wilson, I. Lawrence, S. Mikkelsen, M.F. Lawrence, Direct detection of the hybridization of synthetic homo-oligomer DNA sequences by field effect, J. Phys. Chem., B 101 (1997) 2980–2985.
[37] H. Korri-Youssoufi, F. Garnier, P. Srivastava, P. Godillot, A. Yassar, Toward bioelectronics: specific DNA recognition based on an oligonucleotide-functionalized polypyrrole, J. Am. Chem. Soc. 119 (1997) 7388–7389.
[38] J. Wang, M. Jiang, A. Fortes, B. Mukherjee, New label-free DNA recognition based on doping nucleic-acid probes within conducting polymer films, Anal. Chim. Acta 402 (1999) 7–12.
[39] L.A. Thompson, J. Kowalik, M. Josowicz, J. Janata, Label-free DNA hybridization probe based on a conducting polymer, J. Am.Chem. Soc. 125 (2003) 324–325.
[40] A. Emge, P. Bauerle, Molecular recognition properties of nucleobase-functionalized polythiophenes, Synth. Met. 102 (1999) 1370–1373.
[41] N. Lassalle, E. Vieil, J.P. Correia, L.M. Abrantes, Study of DNA hybridization by photocurrent spectroscopy, Synth. Met. 119 (2001) 407–408.
[42] J. Cha, J.I. Han, Y. Choi, D.S. Yoon, K.W. Oh, G. Lim, DNA hybridization electrochemical sensor using conducting polymer, Biosens. Bioelectron. 18 (2003) 1241–1247.
[43] H. Peng, C. Soeller, P.A. Vigar, M.B. Kilmartin, G.A. Cannell, R.P. Bowmaker, J. Cooney, Label-free electrochemical DNA sensor based on functionalised conducting copolymer, Biosens. Bioelectron. 20 (2005) 1821–1828.
[44] M.C. Pham, B. Piro, L.D. Tran, T. Ledoan, L.H. Dao, Direct electrochemical detection of oligonucleotide hybridization on poly(5-hydroxy-1,4-naphthoquinone-co-5-hydroxy-3-thioacetic acid-1,4-naphthoquinone) film, Anal. Chem. 75 (2003) 6748–6752.
[45] S. Reisberg, B. Piro, V. Noël, M.C. Pham, DNA electrochemical sensor based on conducting polymer: dependence of the “signal-on” detection on the probe sequence localization, Anal. Chem. 77 (2005) 3351–3356.
[46] E.M. Boon, D.M. Ceres, T.G. Drummond, L.G. Hill, J.K. Barton, Mutation detection by electrocatalysis at DNA-modified electrodes, Nat. Biotechnol. 18 (2000) 1196–1200.
[47] H. Miyahara, K. Yamashita, M. Kanai, K. Uchita, M. Takagi, H. Kondo, S. Takenata, Electrochemical analysis of single nucleotide polymorphisms of p53 gene, Talanta 56 (2002) 829–835.
[48] B. Piro, J. Haccoun, M.C. Pham, L.D. Tran, A. Rubin, H. Perrot, C. Gabrielli, Study of the DNA hybridization transduction behavior of a quinone-containing electroactive polymer by cyclic voltammetry and electrochemical impedance spectroscopy, J. Electronal. Chem. 577 (2005) 155–165.
[49] D.Y. Petrovykh, M.J. H.Kimura-Suda, L.J. Tarlov, Quantitative characterization of DNA films by X-ray photoelectron spectroscopy, Langmuir 20 (2004) 429–440.
[50] B. Saoudi, N. Jammul, M.A. Abel, M.M. Chehimi, G. Dodin, DNA adsorption onto conducting polypyrrole, Synth. Met. 87 (1997) 97–103.